Nonlinear Dyn
DOI 10.1007/s11071-015-1954-z

ORIGINAL PAPER

Dynamical behaviors and soliton solutions of a generalized higher-order nonlinear Schrödinger equation in optical fibers

Min Li · Tao Xu · Lei Wang

Received: 9 November 2014 / Accepted: 31 January 2015

Abstract Under study in this paper is a generalized higher-order nonlinear Schrödinger (GHNLS) equation with the third-order dispersion (TOD), self-steeping (SS) and stimulated Raman scattering effects , which describes the propagation of ultrashort pulses in optical fibers. Via the phase plane analysis, both the homoclinic and heteroclinic orbits are found in the two-dimensional plane autonomous system reduced from the GHNLS equation, which proves the existence of bright and dark soliton solutions from the viewpoint of nonlinear dynamics. Furthermore, through the method of binary Bell polynomials and auxiliary function, the explicit bright and dark soliton solutions under certain conditions are obtained. Particular analysis is made to study the effects of the higher-order on the double-hump bright and double-hole dark solitons. The results show that the self-phase modulation and SS parameters determine the interval between two humps for the double-hump bright soliton, while the one for the double-hole dark soliton is related with the TOD and SS effects. Moreover, numerical simulations show that the double-hump bright soliton and the double-hole dark soliton are more stable when the amplitude or depth is comparably small.

Keywords Generalized higher-order nonlinear Schrödinger equation · Dynamical behaviors · Soliton solutions · Binary Bell polynomials · Numerical simulations

M. Li (✉) · L. Wang
Department of Mathematics and Physics, North China Electric Power University, Beijing 102206, China
e-mail: micheller85@126.com

T. Xu (✉)
College of Science, China University of Petroleum, Beijing 102249, China
e-mail: xutao@cup.edu.cn

1 Introduction

Optical signal processing has been an essential technique in the optical communication system because of its ultrafast response time [1]. If all-optical signal processing only utilize the nonlinear index of refraction, partial signal may be lost due to the nonuniform intensity distribution within the pulse [2]. With the balance between the effects of the group velocity dispersion (GVD) and self-phase modulation (SPM), optical solitons as one kind of solitary waves can improve the system performance due to their stable propagation along optical fibers [3]. The existence of solitons in optical fibers has been demonstrated theoretically [4,5] and observed experimentally [6,7].

The slowly varying electromagnetic waves in optical fibers are usually described by the nonlinear Schrödinger (NLS) equation [8]. However, for the ultrashort pulse propagation in the high-bit-rate and long-distance communication, some higher-order linear and nonlinear terms need to be incorporated into the NLS equation [8]. When the pulse width is less than

Published online: 11 February 2015

100 fs, it is necessary to consider such higher-order effects as the third-order dispersion (TOD), self-steepening (SS) and stimulated Raman scattering (SRS) [9,10]. Of those effects, the TOD can make the asymmetrical temporal broadening [8], the SS is responsible for the asymmetrical spectral broadening [11], and the SRS can account for the self-frequency shift in the femtosecond regime [12]. With the inclusion of the above three higher-order effects, Kodama and Hasegawa derived the generalized higher-order NLS equation [11,13–26]:

$$i\,q_z + \alpha_1\,q_{tt} + \alpha_2|q|^2 q + i\,\varepsilon\Big[\alpha_3\,q_{ttt} + \alpha_4|q|^2 q_t + \alpha_5\,q(|q|^2)_t\Big] = 0, \qquad (1)$$

where $q = q(z,t)$ is the slowly varying envelope of the electric field, z and t are the normalized distance along the direction of the propagation and retarded time, ε denotes the ratio of the width of the spectra to the carrier frequency, and $\alpha_1, \alpha_2, \alpha_3, \alpha_4$ and α_5 are all real parameters that are related to the effects of GVD, SPM, TOD, SS and SRS in optical fibers, respectively.

The integrability of Eq. (1) has been studied from different points of view, like the inverse scattering transform[14], prolongation structure analysis [15,16] and Painlevé analysis [11,17]. With $\alpha_3 \neq 0$, it has been shown that Eq. (1) admits two integrable cases. One is the Hirota equation with $3\alpha_2\alpha_3 = \alpha_1\alpha_4$ and $\alpha_5 = 0$. In this case, solutions and integrable properties have been obtained [18]. The other one is the Sasa-Satsuma equation when the parameters in Eq. (1) satisfy the conditions $3\alpha_2\alpha_3 = \alpha_1\alpha_4$ and $2\alpha_5 - \alpha_4 = 0$ [19]. Bright and dark solitons (corresponding $\alpha_3\alpha_4 > 0$ and $\alpha_3\alpha_4 < 0$) solutions for some special cases of Eq. (1) have been obtained by the inverse scattering transform, Darboux transformation, Hirota method and unified transform method [20–25]. Recently, the breather and double-hump soliton solutions of the Sasa-Satsuma equation have been obtained via the general Darboux transformation, and the shape-changing soliton–breather collision phenomena have been revealed [26]. In addition, the W-shaped soliton solution of the Sasa-Satsuma equation has been studied analytically and numerically[27].

On the other hand, the theory of dynamical system is a subject to study the time evolution rule of system [28]. The nonlinear evolution equation (NLEE) is also used to describe the evolution of waves with the time [29–31]. Soliton solutions of the NLEE can be studied via the homoclinic and heteroclinic orbits of the ordinary differential equations derived from the NLEE [32]. Moreover, the changes of the parameters in the NLEE can influence the dynamical behaviors of the system, which may lead to the new types of solitons [33]. Therefore, the dynamical system can be used to study and verify some properties of soliton solutions of the NLEE.

Since Eq. (1) admits several different types of soliton structures, in this paper we plan to study its soliton solutions from the viewpoint of dynamical system, which can further prove the existence of soliton solutions. In Sect. 2, we will analyze the fixed points and phase portraits for the nonlinear ordinary differential system reduced from Eq. (1) and point out that such equation possesses both bright and dark soliton solutions. Although the bright and dark solitons of Eq. (1) have been obtained, the dynamics of the double-hump and double-hole soliton profiles have not yet been analyzed in detail. It has been found that such kind of solitons may allow higher-bit-rate transmission systems based on the multilevel information coding scheme in each pulse [34]. Therefore, in Sect. 3, we will derive the double-hump bright soliton and double-hole dark soliton solutions via the method of binary Bell polynomials and auxiliary function. Meanwhile, we will discuss the relevance of the higher-order effects with the interval between two centers of the double-hump soliton or two holes of the double-hole dark soliton. In Sect. 4, we will analyze the stability of those two types of solitons via the numerical simulations. Section 5 will be our conclusions.

2 Phase plane analysis of Eq. (1)

Dynamical behaviors of the phase orbits near the equilibrium points can reflect the types of solutions for the ordinary differential equation [32,33]. Usually, homoclinic and heteroclinic orbits of nonlinear ordinary differential equations (NODEs) correspond to the bell-shaped and kink-shaped soliton solutions [33]. For the nonlinear partial differential equations (NPDEs) with the complex dependent variables, homoclinic and heteroclinic orbits of the NODEs derived from the NPDEs indicate the existence of the bright and dark soliton solutions [33]. In the following, we will make the phase plane analysis based on the traveling wave solutions of Eq. (1).

By introducing the traveling wave transformation,

$$q(z,t) = \phi(\xi) e^{i\,\Theta}\,,\ \xi = a(t - c\,z)\,,\ \Theta = K\,t - \Omega\,z\,, \tag{2}$$

we transform Eq. (1) into the following form,

$$\begin{aligned} i\,[a^3\varepsilon\alpha_3\phi''' + a\,\varepsilon\,(\alpha_4 + 2\,\alpha_5)\phi^2\phi' - (a\,c - 2\,a\,K\,\alpha_1 \\ + 3\,a\,K^2\,\varepsilon\,\alpha_3)\phi'] + [(a^2\alpha_1 - 3a^2K\varepsilon\alpha_3)\phi'' + (\Omega \\ - K^2\alpha_1 + K^3\varepsilon\alpha_3)\phi + (\alpha_2 - K\varepsilon\alpha_4)\phi^3] = 0 \end{aligned} \tag{3}$$

where a, c, K and Ω are the real constants, $\phi(\xi)$ is a real-value function of ξ, and the prime means the differentiation with respect to the new variable ξ.

Equating the real and imaginary parts of Eq. (3) yields the following two equations:

$$\begin{aligned} a^3\varepsilon\alpha_3\phi''' + a\,\varepsilon\,(\alpha_4 + 2\,\alpha_5)\phi^2\phi' \\ - (a\,c - 2\,a\,K\,\alpha_1 + 3\,a\,K^2\,\varepsilon\,\alpha_3)\phi' = 0\,, \end{aligned} \tag{4a}$$

$$\begin{aligned} (a^2\alpha_1 - 3a^2K\varepsilon\alpha_3)\phi'' + (\Omega - K^2\alpha_1 + K^3\varepsilon\alpha_3)\phi \\ + (\alpha_2 - K\varepsilon\alpha_4)\phi^3 = 0\,. \end{aligned} \tag{4b}$$

Integrating Eq. (4a) and taking integration constant as zero gives

$$\begin{aligned} a^3\varepsilon\,\alpha_3\,\phi'' + a\,(2K\alpha_1 - 3\,K^3\varepsilon\alpha_3 - c)\phi \\ + \frac{1}{3}\,a\,\varepsilon\,(\alpha_4 + 2\,\alpha_5)\phi^3 = 0\,. \end{aligned} \tag{5}$$

In order to make Eq. (4b) and Eq. (5) compatible, we obtain K and Ω as follows:

$$K = \frac{\alpha_1\alpha_4 - 3\alpha_2\alpha_3 + 2\alpha_1\alpha_5}{6\varepsilon\,\alpha_3\alpha_5}\,, \tag{6a}$$

$$\Omega = \frac{2K\,\alpha_1^2 - \alpha_1(c + 8K^2\varepsilon\,\alpha_3)}{\varepsilon\,\alpha_3} + K\,(3c + 8K^2\varepsilon\alpha_3)\,. \tag{6b}$$

As a result, Eq. (4a) and Eq. (4b) are reduced to the following ordinary differential equation:

$$\beta_1\,\phi'' + \beta_2\,\phi + \beta_3\,\phi^3 = 0\,, \tag{7}$$

with

$$\beta_1 = \frac{a^2(3\,\alpha_2\alpha_3 - \alpha_1\alpha_4)}{2\alpha_5}\,, \tag{8}$$

$$\begin{aligned} \beta_2 = -(3\alpha_2\alpha_3 - \alpha_1\alpha_4) \\ \times \frac{(3\alpha_2\alpha_3 - \alpha_1\alpha_4)^2 + 4c\alpha_5^2(3\varepsilon\alpha_3 - \alpha_1^2)}{24\varepsilon^2\alpha_3^2\alpha_5^3}\,, \end{aligned} \tag{9}$$

$$\beta_3 = \frac{(3\alpha_2\alpha_3 - \alpha_1\alpha_4)(\alpha_4 + 2\alpha_5)}{6\alpha_3\alpha_5}\,. \tag{10}$$

Taking $X \equiv \phi$, $Y \equiv \phi_\xi$, we can rewrite Eq. (7) into the two-dimensional plane autonomous system:

$$\begin{aligned} X' &= Y\,, \\ Y' &= -\frac{\beta_2}{\beta_1}X - \frac{\beta_3}{\beta_1}X^3\,, \end{aligned} \tag{11}$$

which is a Hamiltonian system with the Hamiltonian function

$$H(X,Y) = \frac{1}{2}Y^2 + \frac{\beta_2}{2\beta_1}X^2 + \frac{\beta_3}{4\beta_1}X^4. \tag{12}$$

To analyze the equilibrium states of System (11), we need to derive the eigenvalues of the Jacobian matrix at the equilibrium points. The Jacobian matrix of System (11) is given as

$$J = \begin{pmatrix} 0 & 1 \\ -\dfrac{\beta_2 + 3\beta_3X^2}{\beta_1} & 0 \end{pmatrix},$$

which yields the following characteristic equation

$$\lambda^2 + \frac{\beta_2 + 3\beta_3X^2}{\beta_1} = 0\,. \tag{13}$$

Solving Eq. (13) leads to the eigenvalue as

$$\lambda_{1,2} = \pm\sqrt{-(\beta_2 + 3\beta_3X^2)/\beta_1}\,.$$

The detailed discussions about the equilibrium points and their stability are presented as follows:

1. In the case of $\beta_2/\beta_3 \geqslant 0$, there is only one equilibrium point $(0, 0)$ and the eigenvalue at this point is $\pm\sqrt{-\beta_2/\beta_1}$. Then, $(0, 0)$ is a center if $\beta_2/\beta_1 > 0$ while $(0, 0)$ is an unstable saddle point if $\beta_2/\beta_1 < 0$.
2. In the case of $\beta_2/\beta_3 < 0$, System (11) has three equilibrium points: $S_0\ (0, 0)$, $S_1\ (\sqrt{-\beta_2/\beta_3}, 0)$ and $S_2\ (-\sqrt{-\beta_2/\beta_3}, 0)$. The eigenvalues at those equilibrium points are $\pm\sqrt{-\beta_2/\beta_1}$, $\pm\sqrt{2\beta_2/\beta_1}$ and $\pm\sqrt{2\beta_2/\beta_1}$, respectively. If $\beta_2/\beta_1 < 0$, S_0 is an unstable saddle point while S_1 and S_2 are both centers, which means that there exist the homoclinic orbits to S_0 enclosing the centers S_1 and S_2. If $\beta_2/\beta_1 > 0$, S_0 is a center while S_1 and S_2 are both unstable saddle points, which indicates that the phase orbits behave in the heteroclinic form.

In order to show the analysis above clearly, the phase portraits of System (11) under the condition $\beta_2/\beta_3 < 0$ are given in Fig. 1. If the parameters are chosen as $\beta_1 = 1/2$, $\beta_2 = -19/8$ and $\beta_3 = 5/6$, one saddle point and two centers can be seen in Fig. 1a. The orbits

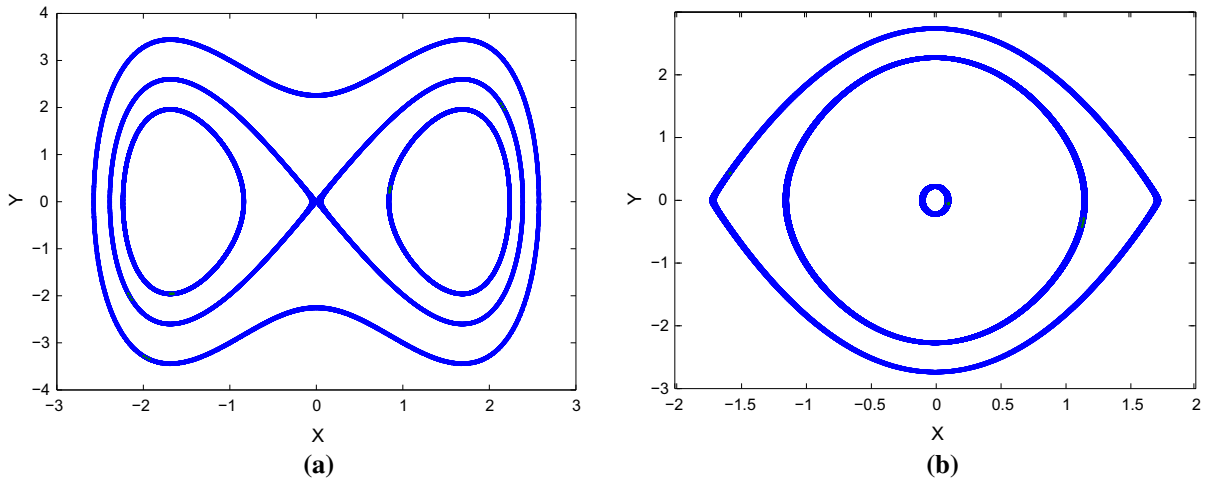

Fig. 1 Phase portraits of System (11): (**a**) homoclinic orbits with $\beta_1 = 1/2,\ \beta_2 = -19/8$ and $\beta_3 = 5/6$; (**b**) heteroclinic orbits with $\beta_1 = -1,\ \beta_2 = -5$ and $\beta_3 = 5/3$

starting from the saddle will finally come back as the time evolves, which form the homoclinic orbits. By choosing $\beta_1 = -1,\ \beta_2 = -5$ and $\beta_3 = 5/3$, we get one center and two saddle points. In this case, two heteroclinic orbits starting from one saddle to another are shown in Fig. 1b.

According to the relationship between the soliton solutions and phase orbits, we find that Eq. (7) admits the bell-shaped soliton solutions if $\beta_2/\beta_3 < 0$ and $\beta_2/\beta_1 < 0$, while the kink-shaped soliton solutions arise if $\beta_2/\beta_3 < 0$ and $\beta_2/\beta_1 > 0$. Note that conditions $\beta_2/\beta_3 < 0$ and $\beta_2/\beta_1 < 0$ can be reduced to the parameter condition $\alpha_3\alpha_4 > 0$ in Eq. (1) via expressions (8), (9) and (10). Similarly, conditions $\beta_2/\beta_3 < 0$ and $\beta_2/\beta_1 > 0$ correspond to the condition $\alpha_3\alpha_4 < 0$ in Eq. (1). It shows that Eq. (1) admits the bright soliton solutions if $\alpha_3\alpha_4 > 0$, while the dark soliton solutions if $\alpha_3\alpha_4 < 0$. Those results are in complete accordance with the previous studies of Eq. (1) via the soliton theory [20–25], which gives the conditions for the bright and dark solitons directly through constructing such solutions.

3 Soliton solutions via the binary Bell polynomials

Based on the analysis of the bright and dark solitons in Sect. 2, we will derive the corresponding explicit soliton solutions via the method of binary Bell polynomials. The key step is to transform Eq. (1) into a linear combination of the binary Bell polynomials via the dependent variable transformation and auxiliary function. Some relevant notations on the Bell polynomials are given in the Appendix.

With the following dependent variable transformation

$$q = e^{u}, \quad q^* = e^{u^*}, \tag{14}$$

where $u = u(z,t)$ is a complex function and the star denotes the complex conjugate, Eq. (1) becomes the following form

$$\begin{aligned} &i\,u_z + \alpha_2 e^{u+u^*} + \alpha_1(u_t^2 + u_{tt}) + i\,\varepsilon[\alpha_3(u_t^3 + 3\,u_t u_{tt} \\ &\quad + u_{ttt}) + \alpha_4 u_t e^{u+u^*} + \alpha_5(u_t + u_t^*)e^{u+u^*}] = 0. \end{aligned} \tag{15}$$

In order to make Eq. (15) be the linear combination of the binary Bell polynomials, we introduce an auxiliary function $v(z,t)$, which is a function of z and t to be determined. Then, we have

$$\begin{aligned} &i\,\mathscr{Y}_z + \alpha_1\mathscr{Y}_{2t} + i\,\varepsilon\,\alpha_3\mathscr{Y}_{3t} - \alpha_1(v_{tt} - u_{tt} - \frac{2\alpha_2}{\alpha_1}e^{u+u^*}) \\ &\quad - i\,\varepsilon\,\alpha_5 e^{u+u^*}(u_t - u_t^*) - \alpha_2 e^{u+u^*} \\ &\quad - i\,\varepsilon\alpha_3 u_t(v_{tt} - u_{tt} - \frac{2\alpha_5 + \alpha_4}{3\alpha_3}e^{u+u^*}) = 0\,. \end{aligned} \tag{16}$$

Under the following condition

$$\frac{2\alpha_2}{\alpha_1} = \frac{2\alpha_5 + \alpha_4}{3\alpha_3}, \tag{17}$$

we get two types of linear binary-Bell-polynomial forms which are, respectively, given as follows:

$$i\,\mathscr{Y}_z(u,v)+\alpha_1\mathscr{Y}_{2t}(u,v)+i\,\varepsilon\,\alpha_3\mathscr{Y}_{3t}(u,v) -e^w=0\,, \tag{18a}$$

$$P_{2t}(v-u)-\frac{2\alpha_2}{\alpha_1}e^{u+u^*}=0\,, \tag{18b}$$

$$i\,\varepsilon\,\alpha_5 e^{u+u^*}\mathscr{Y}_t(u-v)+\alpha_2 e^{u+u^*}-e^w=0, \tag{18c}$$

and

$$i\,\mathscr{Y}_z(u,v)+\alpha_1\mathscr{Y}_{2t}(u,v)+i\,\varepsilon\,\alpha_3\mathscr{Y}_{3t}(u,v) -3\,i\,\varepsilon\,\alpha_3\gamma\,\mathscr{Y}_t(u,v)-e^w-\gamma\,\alpha_1=0\,, \tag{19a}$$

$$P_{2t}(v-u)-\frac{2\alpha_2}{\alpha_1}e^{u+u^*}-\gamma=0\,, \tag{19b}$$

$$i\,\varepsilon\,\alpha_5 e^{u+u^*}\mathscr{Y}_t(u-v)+\alpha_2 e^{u+u^*}-e^w=0, \tag{19c}$$

where $w=w(z,t)$ is an auxiliary function and P_{2t} is defined in Eq. (42).

It is known that there exits the relationship between the $\mathscr{Y}$-polynomial and Hirota D-operator given in Eq. (43). Via the dependent variable transformations

$$u=\ln\frac{g}{f}\,,\quad v=\ln(g\,f)\,,\quad w=\ln\frac{s}{f}, \tag{20}$$

two types of bilinear forms of Eq. (1) are derived as below,

$$\left(i\,D_z+\alpha_1 D_t^2+i\,\varepsilon\,\alpha_3 D_t^3\right)(g\cdot f)-s\,g=0\,, \tag{21a}$$

$$D_t^2(f\cdot f)-\frac{2\alpha_2}{\alpha_1}|g|^2=0\,, \tag{21b}$$

$$i\,\varepsilon\alpha_5 D_t(g\cdot g^*)+\alpha_2|g|^2-s\,f=0\,, \tag{21c}$$

and

$$\left(i\,D_z+\alpha_1 D_t^2+i\,\varepsilon\,\alpha_3 D_t^3 -3\,i\,\varepsilon\,\alpha_3\gamma\,D_t-\gamma\,\alpha_1\right)(g\cdot f)-s\,g=0\,, \tag{22a}$$

$$(D_t^2-\gamma)(f\cdot f)-\frac{2\alpha_2}{\alpha_1}|g|^2=0\,, \tag{22b}$$

$$i\,\varepsilon\alpha_5 D_t(g\cdot g^*)+\alpha_2|g|^2-s\,f=0\,, \tag{22c}$$

with $g=g(z,t)$ as a complex-valued function, $f=f(z,t)$ and $s=s(z,t)$ as the real-value functions, γ as a constant, while D_t and D_z being the bilinear differential operators [35] defined by

$$D_z^m D_t^n(a(z,t)\cdot b(z,t))=\left(\frac{\partial}{\partial z}-\frac{\partial}{\partial z'}\right)^m \times\left(\frac{\partial}{\partial t}-\frac{\partial}{\partial t'}\right)^n a(z,t)\,b(z,t)\Big|_{z'=z,\,t'=t},$$

where $a(z,t)$ and $b(z,t)$ are both differentiable, z' and t' are the independent variables, and m and n are non-negative integers.

3.1 Bright soliton solution

To obtain the bright soliton solutions of Eq. (1), we expand g, f and s with respect to a formal expansion parameter ϵ as

$$g=\epsilon g_1+\epsilon^3 g_3+\epsilon^5 g_5+\epsilon^7 g_7+\cdots\,, \tag{23a}$$

$$f=1+\epsilon^2 f_2+\epsilon^4 f_4+\epsilon^6 f_6+\epsilon^8 f_8+\cdots\,, \tag{23b}$$

$$s=\epsilon^2 s_2+\epsilon^4 s_4+\epsilon^6 s_6+\epsilon^8 s_8+\cdots\,, \tag{23c}$$

where g_l's ($l=1,3,5,\cdots$) are the complex-valued differentiable functions with respect to z and t, f_m's and s_m's ($m=2,4,6\cdots$) are the real-valued differentiable functions with respect to z and t. Substituting Eq. (23) into Bilinear Form (21) and collecting the terms of the same powers of ϵ, we can obtain the recursion relations for g_l's, f_m's and s_m's.

Truncating Eq. (23) as

$$g=\epsilon g_1+\epsilon^3 g_3\,,\quad f=1+\epsilon^2 f_2+\epsilon^4 f_4\,, \quad s=\epsilon^2 s_2+\epsilon^4 s_4 \tag{24}$$

and solving Bilinear Form (21) under the following condition

$$\alpha_1\alpha_4=3\,\alpha_2\alpha_3\,, \tag{25}$$

we derive the bright one-soliton solution

$$q=\frac{g_1+g_3}{1+f_2+f_4} \tag{26}$$

with

$$g_1=e^{\theta}\,,\ g_3=\zeta\,e^{2\theta+\theta^*}\,,\ f_2=\chi\,e^{\theta+\theta^*}\,,\ f_4=\xi\,e^{2\theta+2\theta^*},$$
$$\theta=k\,t+w\,z\,,\quad w=\frac{3i\,\alpha_2\alpha_3k^2-\varepsilon\,\alpha_3\alpha_4k^3}{\alpha_4}\,,$$
$$\zeta=\frac{\alpha_4[2i\alpha_2-\varepsilon\,\alpha_4(k-k^*)]}{12\,\alpha_3(i\alpha_2-\varepsilon\,k\,\alpha_4)(k+k^*)^2}\,,\ \chi=\frac{\alpha_4}{3\alpha_3(k+k^*)^2}\,,$$
$$\xi=-\frac{\alpha_4^2[-2\,i\,\alpha_2+\varepsilon\alpha_4(k-k^*)]^2}{144\alpha_3^2(\alpha_2+i\,\varepsilon\alpha_4k)(\alpha_2-i\,\varepsilon\alpha_4k^*)(k+k^*)^4}\,,$$

where k is a complex constant. To ensure that Solution (26) has no singular points, the condition $\alpha_3\alpha_4>0$ should be satisfied.

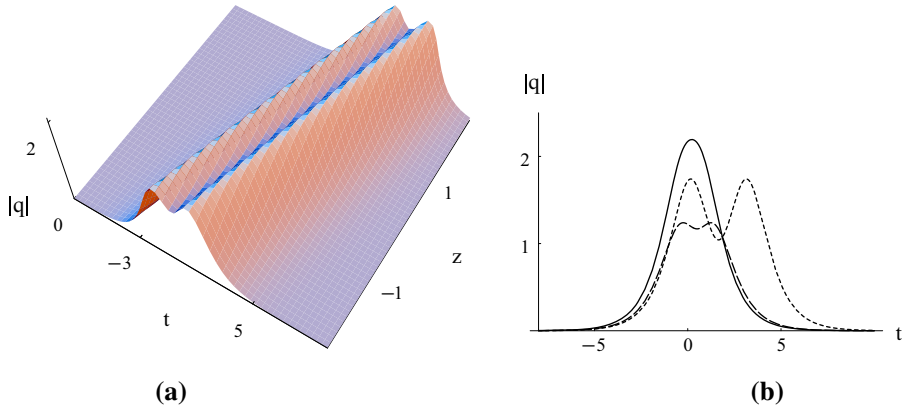

Fig. 2 (**a**) Intensity plot of a double-hump bright soliton by Solution (26) with $\varepsilon = 1$, $k = 1 + 0.1i$, $\alpha_3 = \alpha_4 = 1$ and $\alpha_2 = 0.3$. (**b**) Transverse plots of the double-hump bright soliton in Fig. 2a at $z = -1$, where different values of α_2 are chosen as 1 (*solid curve*), 2.2 (*long dashed curve*) and 0.2 (*short dashed curve*)

Through the extremum analysis of the square modulus of q in Eq. (26), we find that Solution (26) can display the symmetric double-hump structure, as shown in Fig. 2, if

$$3\alpha_2^2 + 3i\varepsilon\alpha_2\alpha_4(k - k^*) - \varepsilon^2\alpha_4^2\left(k^2 - kk^* + k^{*2}\right) < 0. \tag{27}$$

Otherwise, Solution (26) will represent the single-hump bright soliton. Hereby, we only concentrate on the properties of the double-hump soliton since the single one is just the general bright soliton. The amplitude for the double-hump soliton can be obtained as follows:

$$A_1 = \frac{1}{2\sqrt{\chi - \zeta - \zeta^*}}. \tag{28}$$

From Fig. 2b, we find that the interval between two humps depends on the parameter values. Therefore, it is necessary to analyze the variation of the interval. Our calculation shows that the interval between the centers of two humps can be exactly characterized by

$$D = \left|\frac{1}{k + k^*} \ln \frac{P + \sqrt{Q}}{P - \sqrt{Q}}\right| \tag{29}$$

with

$$P = -2\zeta + \chi - 2\zeta^*,$$
$$Q = -4|\zeta|^2 + (2\zeta - \chi + 2\zeta^*)^2.$$

Expression (29) suggests that the interval D is related with the SPM parameter α_2, TOD parameter α_3 and SS parameter α_4. With $\alpha_3 = \alpha_4 = 1$, the variation of D with α_2 is displayed in Fig. 3a, which shows that the interval D decreases as the absolute value of α_2 increases when $|\alpha_1| \geqslant 1$. Differently, the dependence of D on the parameter α_3 is irregular and weak, as shown in Fig. 3b. Figure 3c illustrates the variation of D with α_4, which indicates that the interval D increases as the absolute value of α_4 increases when $|\alpha_4| \geqslant 1.75$. Accordingly, the interval between the centers of two humps can be controlled by modifying the SPM and SS parameters.

3.2 Dark soliton solution

In order to obtain the dark soliton solution of Eq. (1), we expand g, f and s with respect to a formal expansion parameter ϵ as

$$g = g_0(1 + \epsilon g_1 + \epsilon^2 g_2 + \epsilon^3 g_3 + \cdots), \tag{30a}$$
$$f = 1 + \epsilon f_1 + \epsilon^2 f_2 + \epsilon^3 f_3 + \cdots, \tag{30b}$$
$$s = \epsilon s_1 + \epsilon^2 s_2 + \epsilon^3 s_3 + \cdots. \tag{30c}$$

Substituting Eq. (30) into Bilinear Form (22) and collecting the terms of the same powers of ϵ, we can obtain the recursion relations for g_l's, f_l's and s_l's ($l = 1, 2, 3, \cdots$).

By truncating Eq. (30) to the order of ϵ^2, i.e.,

$$g = g_0(1 + \epsilon g_1 + \epsilon^2 g_2), \quad f = 1 + \epsilon f_1 + \epsilon^2 f_2, \quad s = \epsilon s_1 + \epsilon^2 s_2 \tag{31}$$

and solving the recursion relations obtained from Bilinear Form (22) under Condition (25), we derive the dark one-soliton solution

$$q = \frac{g_0(1 + g_1 + g_2)}{1 + f_1 + f_2}, \tag{32}$$

where

$$g_0 = \delta\, e^{i(bt + dz)}, \quad g_1 = \vartheta\, e^{\theta}, \quad g_2 = \mu\, e^{2\theta},$$
$$f_1 = \nu\, e^{\theta}, \quad f_2 = \mu\, e^{2\theta}, \quad \theta = kt + wz,$$
$$w = -\frac{3\alpha_2^2\alpha_3}{\varepsilon\,\alpha_4} - k^2\varepsilon\,\alpha_3 - 2|\delta|^2\varepsilon\alpha_4, \quad b = \frac{\alpha_2}{\varepsilon\,\alpha_4},$$

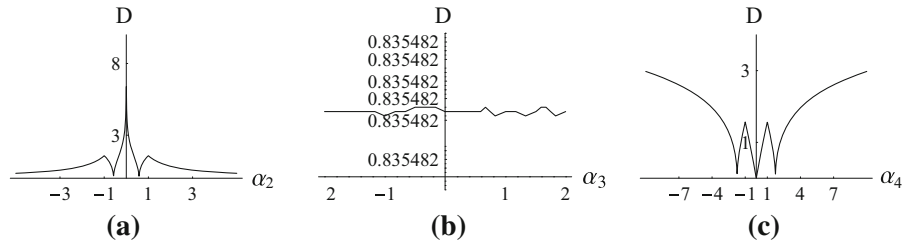

Fig. 3 Variation of the interval between two humps with the SPM parameter α_2, the TOD parameter α_3 and the SS parameter α_4, where (**a**) $\varepsilon = k = \alpha_3 = \alpha_4 = 1$; (**b**) $\varepsilon = k = \alpha_4 = 1$ and $\alpha_2 = 2$; (**c**) $\varepsilon = k = \alpha_2 = \alpha_3 = 1$

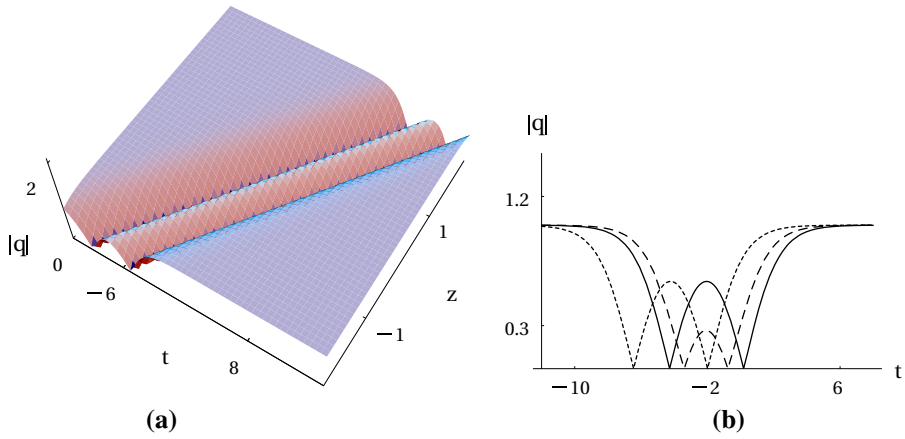

Fig. 4 (**a**) Intensity plot of a double-hole dark soliton by Solution (32) with $\varepsilon = \delta = \zeta = k = 1$, $\alpha_1 = \alpha_2 = \alpha_3 = 1$ and $\alpha_4 = -0.78$. (**b**) Transverse plots of a double-hole dark soliton at $z = -1$ where the parameters are chosen the same as (a) for the *solid curve*, except $\alpha_3 = 0.9$ for the *long dashed curve* and except $\alpha_2 = 1.2$ for the *short dashed curve*

$$d = -\frac{2\,\alpha_2^3\alpha_3}{\varepsilon^2\alpha_4^3}\,,\quad \gamma = -\frac{2|\delta|^2\alpha_4}{\alpha_3}\,,\quad \vartheta = \nu + \frac{3\nu\,\alpha_3 k^2}{2|\delta|^2\alpha_4},$$
$$\mu = \frac{3\nu^2k^2\alpha_3 + 4|\delta|^2\nu^2\alpha_4}{16|\delta|^2\alpha_4}\,,$$

where k and ν are both real constants, while δ is a complex one.

If $\alpha_3(k^2\alpha_3 + |\delta|^2\alpha_4) \leqslant 0$ and $\alpha_3\alpha_4 < 0$, Solution (32) describes the usual dark soliton under the continuous wave background. However, under the following conditions

$$\alpha_3\alpha_4 < 0\,,\quad \alpha_3(k^2\alpha_3 + |\delta|^2\alpha_4) > 0\,,$$
$$\alpha_4(3k^2\alpha_3 + 4|\delta|^2\alpha_4) > 0, \tag{33}$$

Solution (32) displays the symmetric double-hole dark soliton, which has two dips beneath the continuous wave background. Moreover, the depth of such soliton can be obtained by setting $t \to \infty$ for a fixed z, that is, $A_2 = \sqrt{|\delta|^2}$. Figure 4a demonstrates the propagation of a double-hole dark soliton with the parameters satisfying Conditions (33). Figure 4b displays three different transverse plots of the double-hole dark soliton with different choices of parameter values. It is found that the centers of two holes are influenced by the TOD and SS parameters, while the SPM parameter only affects the position of the double-hole dark soliton, which is different from the case of the double-hump bright soliton.

In order to make a quantitative analysis to support the above results, we derive the explicit expression for the interval between two centers of the double-hole dark soliton, that is,

$$D = \left|\frac{1}{k}\ln\frac{P + 3\sqrt{Q}}{P - 3\sqrt{Q}}\right| \tag{34}$$

with

$$P = -3\zeta\alpha_3k^2 - 2\,|\delta|^2\zeta\alpha_4\,,$$
$$Q = \zeta^2k^2\alpha_3(k^2\alpha_3 + |\delta|^2\alpha_4)\,.$$

It is seen from Expression (34) that the interval D is related with the TOD parameter α_3 and SS parameter α_4. The relationship between D and α_3 is illustrated in Fig. 5a, where α_3 ranges from $-4/3$ to -1 to satisfy Conditions (33) and other parameters are all chosen the same as Fig. 1. The interval D decreases as the value of α_3 increases. Figure 5b describes the variation of D with α_4, the range of which is from -1 to $-3/4$ to satisfy Conditions (33) if other parameters are all chosen the same as Fig. 1. Different from the effect of α_3, the interval D increases as the value of α_4 increases. Therefore, we can modify the interval between two centers

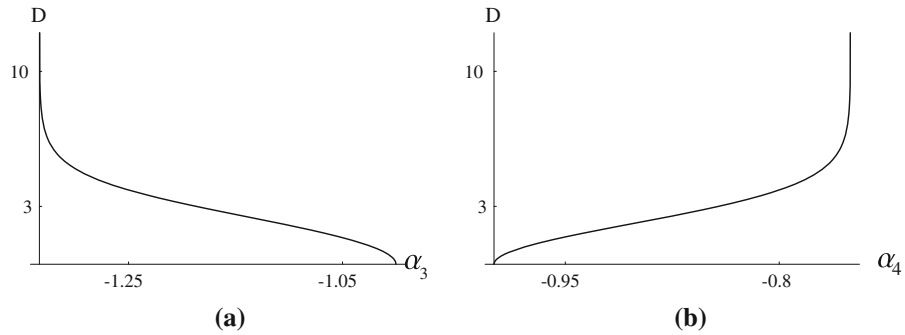

Fig. 5 Variation of the interval of the centers of two humps with the TOD parameter α_3 and the SS parameter α_4, where the parameters are chosen as (**a**) $\zeta = k = 1$, $\alpha_3 = \delta = 1$ and (**b**) $\zeta = k = \alpha_4 = \delta = 1$

of the double-hole dark soliton by changing the values of α_3 and α_4.

4 Numerical simulation and stability analysis

In this section, the stability of the double-hump bright soliton and double-hole dark soliton will be analyzed by the direct numerical simulations. Considering the inclusion of the higher-order nonlinear terms in Eq. (1), we will perform the numerical simulations by the time-splitting spectral (TSS) method, which is regarded as a combination of the time-splitting discretization and Fourier spectral methods and has been successfully applied to the NLS-type equations [38,39]. In particular, at the second step of dealing with the nonlinear equation, we will adopt a fourth-order Runge–Kutta method instead of the direct integral about z to improve the accuracy because the fourth-order Runge–Kutta method exhibits the superior conservation of energy and other invariants [40].

For the double-hump bright soliton, we choose Solution (26) at $z = 0$ as the initial pulse, that is,

$$q(0,t) = \frac{e^{kt} + \zeta e^{(2k+k^*)t}}{1 + \chi e^{(k+k^*)t} + \xi e^{2(k+k^*)t}}, \tag{35}$$

where ζ, χ and ξ are the same as those in Solution (26). By the TSS method, the propagations of the double-hump bright solitons with the specific choices of parameters are simulated, as seen in Fig. 6. It is found that the stability of the double-hump bright soliton is related to the amplitude. When the amplitude is smaller enough, the stable propagation can be obtained in Fig. 6a, where the amplitude is 0.017 given by Expression (28). However, when the amplitude of the double-hump bright soliton increases to 0.022, the propagation will be unstable as the distance z evolves, as seen in Fig. 6b.

By choosing the initial pulse as Solution (32) at $z = 0$, i.e.,

$$q(0,t) = \frac{\delta e^{ibt}(1 + \vartheta e^{kt} + \mu e^{2kt})}{(1 + \nu e^{kt} + \mu e^{2kt})}, \tag{36}$$

where the parameters δ, ϑ, μ and ν are chosen the same as those in Solution (32); the propagations of the double-hole dark solitons are simulated, as seen in Fig. 7. Similarly, the double-hole dark soliton is more stable if the depth is small. When the depth is 0.1, we can get the stable propagation of the double-hole dark soliton in Fig. 7a, while it will become unstable for the depth 0.2 as seen in Fig. 7b.

5 Conclusions

In this paper, we have studied a generalized higher-order nonlinear Schrödinger equation, i.e., Eq. (1), which can describe the propagation of the ultrashort pulses in optical fibers. Phase plane analysis has been performed to study the dynamical behaviors of the ordinary differential equation [i.e., Eq. (7)] derived from Eq. (1), which further proves the existence of bright and dark solitons and provides the corresponding parametric conditions. Via the method of binary Bell polynomials and auxiliary function, we have obtained and analyzed the bright and dark soliton solutions, i.e., Solutions (26) and (32) of Eq. (1). Attentions should be paid to the following aspects:

1. System (11) equivalent to Eq. (7) has been found to possess three equilibrium points under the condition $\beta_2/\beta_3 < 0$. If $\beta_2/\beta_1 < 0$, there exist two homoclinic orbits in the phase portrait containing an unstable saddle point and two centers, as seen in Fig. 1, while the condition $\beta_2/\beta_1 > 0$ leads to two heteroclinic orbits consisting of a center and two unstable saddle points, as seen in Fig. 1b.

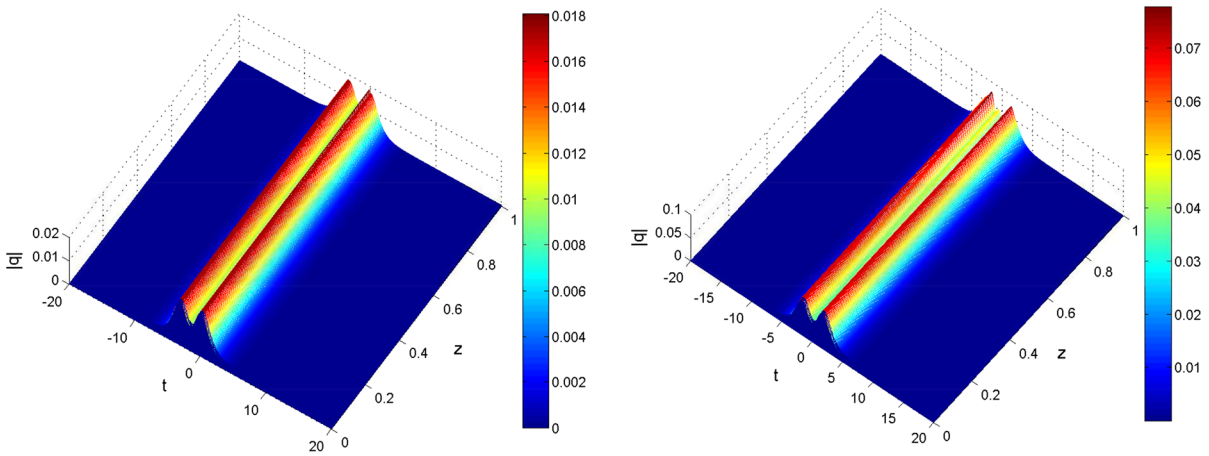

Fig. 6 Numerical simulations on the double-hump bright solitons: (**a**) stable propagation with $\varepsilon = 1,\ k = 1+0.1i,\ \alpha_3 = 0.001,\ \alpha_4 = 10$ and $\alpha_2 = 0.2$; (**b**) unstable propagation with $\varepsilon = 1,\ k = 1+0.1i,\ \alpha_3 = 0.01,\ \alpha_4 = 6$ and $\alpha_2 = 0.2$

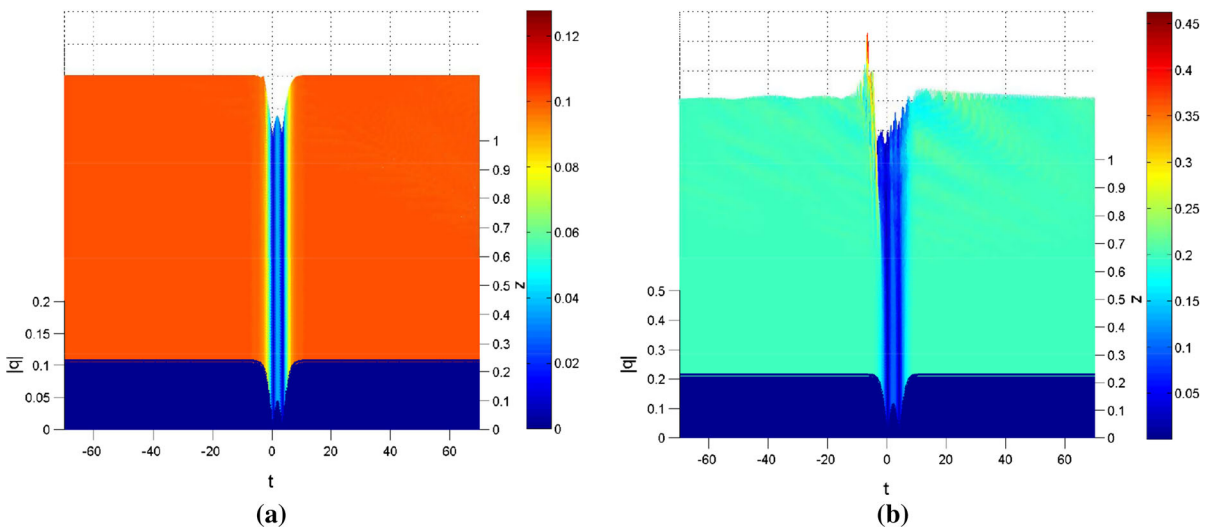

Fig. 7 Numerical simulations on the double-hole dark solitons: (**a**) stable propagation with $\varepsilon = 1,\ k = 1,\ \alpha_3 = 0.12,\ \alpha_4 = -10,\ \alpha_2 = 1,\ \nu = 1$ and $\delta = 0.1$; (**b**) unstable propagation with $\varepsilon = 1,\ k = 1,\ \alpha_3 = 0.2,\ \alpha_4 = -4,\ \alpha_2 = 1,\ \nu = 1$ and $\delta = 0.2$

2. Phase plane analysis has shown that Eq. (7) admits the bell-shaped and kink-shaped soliton solutions, which correspond to the bright and dark soliton solutions of Eq. (1) under the conditions $\alpha_3\alpha_4 > 0$ and $\alpha_3\alpha_4 < 0$, respectively. Those results are in complete accordance with the previous studies of Eq. (1) via the soliton theory [20–25].
3. Through the extremum analysis of the square modulus of q, we have found that the double-hump bright soliton and double-hole dark soliton can occur when the parameters satisfy Conditions (27) and (33), respectively, as shown in Figs. 2 and 4.
4. The explicit Expressions (29) and (34) have been given to characterize the influence of the higher-order effects on the interval between two centers of the double-hump bright soliton and double-hole dark soliton, respectively. The variation of the SPM and SS parameters can affect the interval for the double-hump bright soliton, as shown in Fig. 3. However, for the double-hole dark one, the interval

is related to the TOD and SS effects, as shown in Fig. 5.

5. The numerical simulations for Eq. (1) show that the double-hump bright soliton or the double-hole dark soliton is more stable if the amplitude or depth is comparably small.

Acknowledgments This work has been supported by the Fundamental Research Funds of the Central Universities (Project Nos. 2014QN30 and 2014ZZD10), by the National Natural Science Foundations of China (Grant Nos. 11426105, 11371371,-11305060, 11271126 and 11247267) and by the Postdoctoral Science Foundation of China (2013M540907).

Appendix

Some necessary notations on the Bell polynomials can be seen as follows:

Let $f = f(x_1, \ldots, x_n)$ be a C^∞ multi-variable function then, the multi-dimensional Bell polynomials can be defined as below [36,37]:

$$Y_{n_1x_1,\ldots,n_lx_l}(f) \equiv Y_{n_1,\ldots,n_l}(f_{r_1x_1,\ldots,r_lx_l}) = e^{-f}\partial_{x_1}^{n_1}\cdots\partial_{x_l}^{n_l}e^{f}, \tag{37}$$

where $f_{r_1x_1,\ldots,r_lx_l} = \partial_{x_1}^{r_1}\cdots\partial_{x_l}^{r_l} f$ $(r_k = 0, \ldots, n_k, k = 1, \ldots, l)$ and $Y_{n_1x_1,\ldots,n_lx_l}(f)$ denotes the multi-variable polynomial with respect to $f_{r_1x_1,\ldots,r_lx_l}$. In particular, for $f = f(x,t)$, the associated two-dimensional Bell polynomials are

$$Y_{2x}(f) = f_{2x} + f_x^2, \quad Y_{x,t}(f) = f_{x,t} + f_x f_t, \tag{38}$$

$$Y_{3x}(f) = f_{3x} + 3f_{2x}f_x + f_x^3, \tag{39}$$

$$Y_{2x,t}(f) = f_{2x,t} + f_{2x}f_t + 2f_{x,t}f_x + f_x^2 f_t, \quad \ldots. \tag{40}$$

In order to differ the odd- and even-order derivatives of $f_{r_1x_1,\ldots,r_lx_l}$, the multi-dimensional binary Bell polynomial ($\mathscr{Y}$-polynomial) is introduced as follows [37]:

$$\mathscr{Y}_{n_1x_1,\ldots,n_lx_l}(v,\omega) = Y_{n_1x_1,\ldots,n_lx_l}(f)\Big|_{f_{r_1x_1,\ldots,r_lx_l}\begin{cases} v_{r_1x_1,\ldots,r_lx_l}, \\ (r_1+\cdots+r_l \text{ is odd}). \\ \omega_{r_1x_1,\ldots,r_lx_l}, \\ (r_1+\cdots+r_l \text{ is even}). \end{cases}}$$

Then, Eqs. (38), (39) and (40) can be rewritten in the form of binary Bell polynomials as

$$\mathscr{Y}_{2x}(v,\omega) = \omega_{2x} + v_x^2, \quad \mathscr{Y}_{x,t}(v,\omega) = \omega_{x,t} + v_x v_t,$$
$$\mathscr{Y}_{3x}(v,\omega) = v_{3x} + 3\omega_{2x}v_x + v_x^3,$$
$$\mathscr{Y}_{2x,t}(v,\omega) = v_{2x,t} + \omega_{2x}v_t + 2\omega_{x,t}v_x + v_x^2 v_t, \quad \ldots.$$

Note that the $\mathscr{Y}$-polynomial and the Hirota expression $D_{x_1}^{n_1}\cdots D_{x_l}^{n_l} F\cdot G$ can be linked by the identity [37]

$$(FG)^{-1}D_{x_1}^{n_1}\cdots D_{x_l}^{n_l}F\cdot G = \mathscr{Y}_{n_1x_1,\ldots,n_lx_l}(v = \ln F/G, \omega = \ln FG), \tag{41}$$

where the Hirota bilinear operators are defined by [35]

$$D_{x_1}^{n_1}\cdots D_{x_l}^{n_l}(F\cdot G) = \left(\frac{\partial}{\partial x_1} - \frac{\partial}{\partial x_1'}\right)^{n_1}\cdots \times \left(\frac{\partial}{\partial x_l} - \frac{\partial}{\partial x_l'}\right)^{n_l} F(x_1,\ldots,x_l) \times G(x_1',\ldots,x_l')\Big|_{x_1'=x_1,\ldots,x_l'=x_l}.$$

In particular, when $F = G$, Eq. (41) becomes

$$(G)^{-2}D_{x_1}^{n_1}\cdots D_{x_l}^{n_l}G\cdot G = \mathscr{Y}_{n_1x_1,\ldots,n_lx_l}(v=0,\omega=2\ln G) = \begin{cases} 0, & n_1+\cdots+n_l \text{ is odd}, \\ P_{n_1x_1,\ldots,n_lx_l}(\omega), & n_1+\cdots+n_l \text{ is even}, \end{cases} \tag{42}$$

where the P-polynomials take the even part partitional structure

$$P_{2x}(\omega) = \omega_{2x}, \quad P_{x,t}(\omega) = \omega_{xt}, \tag{43}$$

$$P_{4x}(\omega) = \omega_{4x} + 3\omega_{2x}^2 \ldots. \tag{44}$$

Therefore, a nonlinear equation can be transformed into the corresponding bilinear equation via Expressions (41), (43) and (44), once this nonlinear equation is expressible as a linear combination of $\mathscr{Y}$-polynomials.

References

1. Watanabe, S.: Optical signal processing using nonlinear fibers. J. Opt. Fiber Commun. Rep. **3**, 1–24 (2006)
2. Willner, A.E., Khaleghi, S., Chitgarha, M.R., Yilmaz, O.F.: All-optical signal processing. J. Light. Tech. **32**, 660–680 (2014)
3. Doran, N.J., Blow, K.J.: Solitons in optical communications. IEEE J. Quan. Electron. **19**, 1883–1888 (1983)
4. Hasegawa, A., Tappert, F.: Transmission of stationary nonlinear optical pulses in dispersive dielectric fibers. I. Anomalous dispersion. Appl. Phys. Lett. **23**, 142 (1973)
5. Hasegawa, A., Tappert, F.: Transmission of stationary nonlinear optical pulses in dispersive dielectric fibers. II. Normal dispersion. Appl. Phys. Lett. **23**, 171 (1973)
6. Mollenauer, L.F., Stolen, R.H., Gordon, J.P.: Experimental observation of picosecond pulse narrowing and solitons in optical fibers. Phys. Rev. Lett. **45**, 1095–1098 (1980)
7. Emplit, P., Hamaide, J.P., Reynaud, F., Froehly, C., Barthelemy, A.: Picosecond steps and dark pulses through nonlinear single mode fibers. Opt. Commun. **62**, 374–379 (1987)

8. Agrawal, G.P.: Nonlinear Fiber Optics. Academic, California (2002)
9. Mitschke, F.M., Mollenauer, L.F.: Random walk of coherently amplified solitons in optical fiber transmission. Opt. Lett. **11**, 665–667 (1986)
10. Gordon, J.P.: Theory of the soliton self-frequency shift. Opt. Lett. **11**, 662–664 (1986)
11. Porsezian, K., Nakkeeran, K.: Optical solitons in presence of Kerr dispersion and self-frequency shift. Phys. Rev. Lett. **76**, 3955–3958 (1996)
12. Kivshar, Yu S., Agrawal, G.P.: Optical Solitons: From Fibers to Photonic Crystals. Academic, San Diego (2003)
13. Porsezian, K.: Soliton models in resonant and nonresonant optical fibers. Pramāna **57**, 1003–1039 (2001)
14. Mihalache, D., Torner, L., Moldoveanu, F., Panoiu, N.C., Truta, N.: Inverse-scattering approach to femtosecond solitons in monomode optical fibers. Phys. Rev. E **48**, 4699–4709 (1993)
15. Gedalin, M., Scott, T., Band, Y.: Optical solitary waves in the higher order nonlinear Schrödinger equation. Phys. Rev. Lett. **78**, 448–451 (1997)
16. Mihalache, D., Truta, N., Crasovan, L.C.: Painlevé analysis and bright solitary waves of the higher-order nonlinear Schrödinger equation containing third-order dispersion and self-steepening term. Phys. Rev. E **56**, 1064–1070 (1997)
17. Nijhof, J.H.B., Roelofs, G.H.M.: Prolongation structures of a higher-order nonlinear Schrödinger equation. J. Phys. A **25**, 2403–2416 (1992)
18. Hirota, R.: Exact envelope-soliton solutions of a nonlinear wave equation. J. Math. Phys. **14**, 805–809 (1973)
19. Sasa, N., Satsuma, J.: New-type of soliton solutions for a higher-order nonlinear Schrödinger equation. J. Phys. Soc. Jpn. **60**, 409–417 (1991)
20. Xu, Z.Y., Li, L., Li, Z.H., Zhou, G.S.: Soliton interaction under the influence of higher-order effects. Opt. Commun. **210**, 375–384 (2002)
21. Gilson, C., Hietarinta, J., Nimmo, J., Ohta, Y.: Sasa-Satsuma higher-order nonlinear Schrödinger equation and its bilinearization and multisoliton solutions. Phys. Rev. E **68**, 016614 (2008)
22. Palacios, S.L., Guinea, A., Fernández, J.M., Crespo, R.D.: Dark solitary waves in the nonlinear Schrödinger equation with third order dispersion, self-steepening, and self-frequency shift. Phys. Rev. E **60**, R45–R47 (1999)
23. Jiang, Y., Tian, B.: Dark and dark-like-bright solitons for a higher-order nonlinear Schrödinger equation in optical fibers. EPL **102**, 10010 (2013)
24. Jiang, Y., Tian, B., Li, M., Wang, P.: Bright hump solitons for the higher-order nonlinear Schröinger equation in optical fibers. Nonlinear Dyn. **74**, 1053–1063 (2013)
25. Xu, J., Fan, E.: The unified transform method for the Sasa-Satsuma equation on the half-line. Proc. R. Soc. A **469**, 20130068 (2013)
26. Xu, T., Wang, D.H., Li, M., Liang, H.: Soliton and breather solutions of the Sasa-Satsuma equation via the Darboux transformation. Phys. Scr. **89**, 075207 (2014)
27. Zhao, L.C., Li, S.C., Ling, L.M.: Rational W-shaped solitons on a continuous-wave background in the Sasa-Satsuma equation. Phys. Rev. E **89**, 023210 (2014)
28. Alligood, K.T., Sauer, T.D., Yorke, J.A.: An Introduction to Dynamical Systems. Springer, Berlin (2000)
29. Ablowitz, M.A., Clarkson, P.A.: Solitons Nonlinear Evolution Equations and Inverse Scattering. Cambridge University, Cambridge (1992)
30. Guo, R., Hao, H.Q.: Breathers and localized solitons for the Hirota–Maxwell–Bloch system on constant backgrounds in erbium doped fibers. Ann. Phys. **344**, 10–16 (2014)
31. Guo, R., Hao, H.Q., Zhang, L.L.: Dynamic behaviors of the breather solutions for the AB system in fluid mechanics. Nonlinear Dyn. **74**, 701–709 (2013)
32. Liu, S.D., Liu, S.K.: Soliton Wave and Turbulence (Chinese version). Shanghai Scientific and Technological Education, Shanghai (1994)
33. Infeld, E., Rowlands, G.: Nolinear Waves Solitons and Chaos. Cambridge University, Cambridge (2000)
34. Akhmediev, N., Ankiewicz, A.: Multi-soliton complexes. Chaos **10**, 600–612 (2000)
35. Hirota, R.: The Direct Method in Soliton Theory. Cambridge University, Cambridge (2004)
36. Lambert, F., Springael, J.: Soliton equations and simple combinatorics. Acta Appl. Math. **102**, 147–178 (2008)
37. Gilson, C., Lambert, F., Nimmo, J., Willox, R.: On the combinatorics of the Hirota D-operators. Proc. R. Soc. Lond. A **452**, 223–234 (1996)
38. Bao, W., Jin, S., Markowich, P.A.: On time-splitting spectral approximations for the Schrödinger equation in the semiclassical regime. J. Comput. Phys. **175**, 487–524 (2002)
39. Bao, W., Jin, S., Markowich, P.A.: Numerical study of time-splitting spectral discretizations of nonlinear Schrödinger equations in the semiclassical regimes. SIAM J. Sci. Comput. **25**, 27–64 (2003)
40. Sanders, B.F., Katopodes, N.D., Boyd, J.P.: Spectral modeling of nonlinear dispersive waves. J. Hydraul. Eng. **124**, 2–12 (1998)